Korea-Australia Rheology Journal
Vol. 21, No. 4, December 2009 pp. 235-244

Component dynamics in miscible polymer blends: A review of recent findings

Hiroshi Watanabe[1,*] and Osamu Urakawa[2]
[1]*Institute for Chemical Research, Kyoto University, Uji, Kyoto 611-0011, Japan*
[2]*Department of Macromolecular Science, Faculty of Science Osaka University, Toyonaka, Osaka 560-0043, Japan*
(Received May 28, 2009)

Abstract

Miscible polymer blends still have heterogeneity in their component chain concentration in the *segmental length scale* because of the chain connectivity (that results in the self-concentration of the segments of respective chains) as well as the dynamic fluctuation over various length scales. As a result, the blend components feel different dynamic environments to exhibit different temperature dependence in their segmental relaxation rates. This type of dynamic heterogeneity often results in a broad glass transition (sometimes seen as two separate transitions), a broad distribution of the local (segmental) relaxation modes, and the thermo-rheological complexity of this distribution. Furthermore, the dynamic heterogeneity also affects the global dynamics in the miscible blends if the component chains therein have a large dynamic asymmetry. Thus, the superficially simple miscible blends exhibit interesting dynamic behavior. This article gives a brief summary of the features of the segmental and global dynamics in those blends.

Keywords : miscible polymer blends, dynamic heterogeneity, self concentration, segmental relaxation, global relaxation, thermo-rheological behavior

1. Introduction

Since polymer chains have very small mixing entropy, chemically different polymers are energetically immiscible in general (Utracki, 1989). However, we also have a considerable number of polymer pairs that exhibit miscibility in given ranges of temperature and composition. Earlier studies appear to have regarded blends of such miscible polymers to be more or less similar to blends of chemically identical polymers thereby placing a rather vague focus on the miscible polymer blends. However, the concentration of the component chains in miscible blends fluctuates over various length/time scales, meaning that these blends are statically homogeneous but dynamically heterogeneous. This dynamic heterogeneity provides the miscible blends with a variety of interesting features such as broad segmental relaxation/glass transition and failure of time-temperature superposition (thermo-rheological complexity) not observed for blends of chemically identical polymers (Miller *et al.*, 1990; Chung *et al.*, 1994; Alegria *et al.*, 1994; Kumar *et al.*, 1996; Miura *et al.*, 2001; Lodge and McLeish, 2000; Pathak *et al.*, 1998, 1999, 2004; Haley *et al.*, 2003; Haley and Lodge, 2005; Hirose *et al.*, 2003, 2004; Urakawa, 2004; Lutz *et al.*, 2004; Ediger *et al.*, 2006; Zhao *et al.*, 2008; Yurekli and Krishnamoorti, 2004; Watanabe *et al.*, 2007; Takada *et al.*, 2008; Chen *et al.*, 2008). This article gives a brief review of these features in the linear viscoelastic regime at equilibrium. The nonlinear features such as the flow-induced phase separation are also very interesting but not described in this article. The readers interested in the nonlinear features are guided to recent papers by Takenaka *et al.* (2006) and by Endoh *et al.* (2008) and the references therein.

2. Local dynamics

2.1. Self concentration

The local dynamics of polymer chains in the length scale of *monomeric* segments governs the glass transition of the chains. Because of this importance, the local dynamics has been extensively investigated experimentally with the thermal, viscoelastic, and dielectric methods. In early studies, polymer blends exhibiting single/sharp and multiple/broad glass transitions were judged to be homogeneous and heterogeneous, respectively. This judgment relies on an assumption that the segments of different component chains feel the same dynamic environment if these chains are homogeneously mixed. In fact, this assumption holds for a lot of systems, as revealed in early experiments (Utracki, 1989).

However, recent experiments indicated that the assumption fails for a considerable number of polymer pairs. For example, blends of *cis*-polyisoprene (PI) and poly(vinyl ethylene) (PVE) exhibit the lower critical solution temperature (LCST) phase behavior, as confirmed from scattering experiments

*Corresponding author: hiroshi@scl.kyoto-u.ac.jp
© 2009 by The Korean Society of Rheology

(Tomlin and Roland, 1992). The segmental mobilities of PI and PVE in the blends are different even in the miscible state at temperatures $T<T_{LCST}$, as revealed from ^{13}C-NMR and 2-dimensional ^{2}H-exchange NMR spectroscopy (Miller *et al.*, 1990; Chung *et al.*, 1994). Correspondingly, the PI/PVE miscible blends exhibited a very broad, almost two-step glass transition in their thermal behavior (Chung *et al.*, 1994). These results demonstrate that the segments of different component chains may feel different dynamic environments even in miscible blends. In other words, the component chains may have different effective glass transition temperatures T_g^{eff} in the miscible blends (Chung *et al.*, 1994).

This difference of T_g^{eff} of the component chains reflects a difference of their mobilities. The glass transition occurs on thermal activation of the segmental motion (micro-Brownian motion around the chain backbone). Since the torsional barrier for the segmental motion differs for chemically different chains, these chains may naturally/intrinsically have different T_g^{eff} in the miscible blends. (This barrier should be determined by the chemical structure of the chain as well as the packing state of the segments in the blends.)

However, it should be emphasized that the torsional barrier is not the only factor that affects T_g^{eff}. In addition, this barrier exists also for low molecular weight (M) compounds and thus its effect on T_g^{eff} is not unique to polymer chains. Concerning this point, Chung *et al.* (1994) and Lodge and McLeish (2000) focused on the self concentration that exclusively results from the connectivity of segments along the chain backbone, the essential structural feature of polymers: The chemically identical segments neighboring along the chain backbone always occupy neighboring volume elements (or sites) in the blends thereby leading to the self concentration. In blends of polymers A and B, an effective volume fraction $\phi_{eff}^{[X]}$ of a segment X (= A or B) in a close vicinity of this segment is larger than a nominal volume fraction $\phi^{[X]}$ (average in the whole blend), and this $\phi_{eff}^{[X]}$ should determine the effective T_g^{eff} of the segment X. Thus, the components A and B exhibit respective glass transitions in A- and B-rich environments (characterized by $\phi_{eff}^{[A]}$ and $\phi_{eff}^{[B]}$) and may have different T_g^{eff} in the miscible blends.

The Lodge-McLeish model (2000) considers that the effective volume fraction $\phi_{eff}^{[X]}$ is given by

$$\phi_{eff}^{[X]} = \phi_{self}^{[X]} + (1-\phi_{self}^{[X]})\phi^{[X]} \quad \text{with X = A, B} \tag{1}$$

where $\phi_{self}^{[X]}$ is the self-concentrated volume fraction of the segment X resulting from the chain connectivity. This $\phi_{self}^{[X]}$ is expressed in terms of the characteristic ratio $C_{\infty}^{[X]}$ of the chain X, molecular weight $M_0^{[X]}$ and the number $k^{[X]}$ of the backbone bonds per repeating unit of the chain, a volume $V_K^{[X]}$ corresponding to the Kuhn length b_K ($V_K^{[X]} \sim b_K^3$), mass density of the blend ρ, and Avogadro constant N_A as

$$\phi_{self}^{[X]} = \frac{C_{\infty}^{[X]} M_0^{[X]}}{k^{[X]} V_K^{[X]} \rho N_A} \quad \text{with X = A, B} \tag{2}$$

We may describe T_g^{eff} as a function of the nominal volume fraction $\phi^{[X]}$ by combining the above expression of $\phi_{eff}^{[X]}$ with an empirical equation that describes the *single* T_g^o in idealized miscible blends with no self concentration, for example, the Fox equation given below.

$$\frac{1}{T_g^o} = \frac{\phi_A}{T_g^{\text{pure A}}} + \frac{\phi_B}{T_g^{\text{pure B}}}$$

(with ϕ_X=volume fraction of X in idealized blend) (3)

From Eqs. (1)-(3), T_g^{eff}(A) and T_g^{eff}(B) of the components A and B subjected to the self concentration effect are expressed as (Lodge and McLeish, 2000)

$$T_g^{eff}(A) = T_g^o(\phi_A = \phi_{eff}^{[A]}),\ T_g^{eff}(B) = T_g^o(\phi_B = \phi_{eff}^{[B]}) \tag{4}$$

For a test of the molecular picture of self concentration, extensive studies have been made, for example, by Chung *et al.* (1994), Pathak *et al.* (1998, 1999), Hirose *et al.*, (2003, 2004), Urakawa (2004), Lutz *et al.* (2004), Ediger *et al.* (2006), and Zhao *et al.* (2008). These studies revealed the basic validity of this picture (for describing changes of T_g^{eff} with the blend composition) together with its *limitation*. Namely, the self-concentrated volume fraction $\phi_{self}^{[X]}$ involved in the Lodge-McLeish model is expressed in terms of the molecular parameters of the chain X and thus intrinsic to this chain (cf. Eq. (2)), while the experimental $\phi_{self}^{[X]}$ obtained from fitting of the T_g^{eff} data with the model changes from system to system. For example, ^{13}C-NMR experiments by Lutz *et al* (2004) indicated that dilute low-M *cis*-polyisoprene (PI) chains have different $\phi_{self}^{[PI]}$ values in miscible matrices of high-M poly(vinyl ethylene) (PVE), poly(1,4-butadiene) (PB), and polystyrene (PS), $\phi_{self}^{[PI]}$ =0.41 (in PVE), 0.85 (in PB), and 0.20 (in PS). The $\phi_{self}^{[PI]}$ value in the PVE matrix is close to the prediction of Eq. (2) ($\phi_{self}^{[PI]}$ =0.45) but those in the PB and PS matrices significantly differ from the prediction.

Thus, factors other than the self concentration need to be incorporated in accurate description of the local, segmental dynamics that governs the glass transition. The factors include the torsional barrier along the chain backbone (as explained earlier) and the motional cooperativity of neighboring segments, the latter being discussed extensively for homopolymer systems (Kanaya and Kaji, 2001). In addition, the segment size itself may change if the system density considerably changes on blending (Inoue *et al.*, 2002), which may also contribute to the deviation from the prediction of the Lodge-McLeish model. Further studies are strongly desired for these factors.

2.2. Length scale of segmental dynamics

The glass transition phenomenon unequivocally reflects thermal activation of the segmental motion, but the size of the monomeric segment itself has been rarely specified. Concerning this problem, Hirose *et al.* (2003, 2004) and

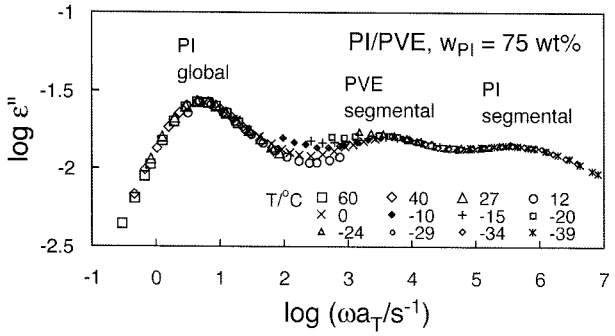

Fig. 1. Master curve of ε" obtained for a PI/PVE blend with $M_{PI}=11.5\times10^3$, $M_{PVE}=60.2\times10^3$ and $w_{PI}=75$ wt%. The reference temperature is $T_r=-20$°C. Data taken from Hirose *et al.* (2003) with permission.

Urakawa (2004) conducted extensive dielectric studies for miscible blends of linear PI and PVE chains. Their results are summarized below.

2.2.1. Analysis based on internal reference of length scale

Both of PI and PVE chains have the so-called type-B dipoles perpendicular to the chain backbone, and PI chains also have the type-A dipoles parallel along the backbone. The dielectric relaxation reflects the fluctuation of these dipoles with time (Watanabe, 2001). Specifically, the local motion of the segments results in the fluctuation of the type-B dipoles attached thereto, enabling us to detect this motion as a fast dielectric relaxation process. In contrast, the sum of the type-A dipoles of the linear PI chain is proportional to the end-to-end vector **R** so that the slow dielectric relaxation of PI exclusively detects the fluctuation of **R**. These dielectric features of PI and PVE are clearly noted in Fig. 1, where a master curve of the dielectric loss (ε") is shown for a PI/PVE blend with the component molecular weights $M_{PI}=11.5\times10^3$ and $M_{PVE}=60.2\times10^3$ and the PI content $w_{PI}=75$ wt% (Hirose *et al.*, 2003). The reference temperature is $T_r=-20$°C. The three distinct dispersions seen at high, middle and low angular frequencies (ω) are attributed to the segmental motion of PI, the segmental motion of PVE, and the global motion of PI, respectively (Hirose *et al.*, 2003; Urakawa, 2004). Note that the PVE chains have no type-A dipole and thus their global motion is dielectrically inert. (However, the global motion of PVE, slower than that of PI, was detected as the terminal viscoelastic relaxation of the blend as a whole.)

In the master curve shown in Fig. 1, the ε" data measured at various temperatures ($-39\le T/$°C≤60) were shifted along the ω axis by an appropriate factor a_T to achieve the best superposition in the segmental and/or global relaxation regime for PI. This shift (for PI) gives very poor superposition in the segmental relaxation regime for PVE, which confirms a difference of the effective T_g^{eff} of the component chains in the blends discussed earlier. Namely, this difference of T_g^{eff} ($T_{g,PVE}^{eff}>T_{g,PI}^{eff}$) leads to a difference of the *iso-frictional* reference temperatures for the WLF-type shift factors a_T for PI and PVE, which results in the failure of the superposition for the blend as a whole. (The temperature dependence of a_T is stronger for PVE having a higher T_g^{eff}).

For the PI/PVE blends, the segmental and global relaxation processes are simultaneously detected (cf. Fig. 1) and the latter process corresponds to the motion of the PI chain over an average end-to-end distance, $R_{PI}=\langle\mathbf{R}^2\rangle^{1/2}$ ($\propto M^{1/2}$). Thus, utilizing R_{PI} as an internal reference of the length scale, we may estimate a length scale for the segmental relaxation of PI by comparing the global and segmental dielectric relaxation times, τ_e and $\tau_{\varepsilon,seg}$. Specifically, for PI chains that have M_{PI} smaller than the characteristic molecular weight for entanglement M_e ($\cong10\times10^3$; Ferry, 1980) and are regarded as the Rouse chain, τ is proportional to $M^2 \sim R_{PI}^4$ and thus the time and length scales $\tau_{\varepsilon,seg}$ and r_{seg} of the segmental relaxation can be correlated to each other as (Hirose et al., 2003)

$$\frac{\tau_{\varepsilon,seg}}{\tau_\varepsilon}=\frac{r_{seg}^4}{R_{PI}^4} \tag{5}$$

This correlation holds for PI in either bulk state or blends with PVE, given that the continuous Rouse relationship underlying Eq. (5), $\tau_{\varepsilon,seg}\propto r_{seg}^4$, is valid. (If r_{seg} is too small, the discrete Rouse relationship is to be utilized instead of the continuous relationship.)

For several PI/PVE blends having $M_{PI}\le M_e$, Hirose *et al.* (2003) utilized the known τ_ε and $\tau_{\varepsilon,seg}$ values (evaluated from the ε" peak frequencies) and the R_{PI} value (evaluated from an empirical equation) in Eq. (5) to estimate the length scale r_{seg} being equivalent to the segment size of PI. The resulting r_{seg} ($=0.9\pm0.04$ nm) was considerably close to the Kuhn segment length of PI, $b_K=0.68$ nm. They also utilized the thermally determined T_g^{eff} data of PI and PVE in PI/PVE blends to reduce the $\tau_{\varepsilon,seg}$ data of PI and PVE in the iso-frictional state and estimated, with the aid of Eq. (5), the r_{seg} value for PVE from the $\tau_{\varepsilon,seg}$ data in this state. The resulting segment size of PVE, $r_{seg}=1.8\pm0.3$ nm, was reasonably close to the Kuhn segment length of PVE, $b_K=1.16$ nm. These results may indicate that the statistically well-defined Kuhn segment behaves as the *dielectrically detected* monomeric segment. (Note that this segment is not necessarily identical to the Rouse segment, the motional unit for the global relaxation of polymer chains; cf. Inoue *et al.*, 2002.)

2.2.2. Analysis based on mode broadening

Hirose *et al.* (2004) further examined the segment size of PVE in PI/PVE blends from analysis of the broadness of the dielectric mode distribution observed as ω dependence of the ε" data. As an example, Fig. 2 shows ω dependence of ε" measured at 10°C for a PI/PVE blend with $M_{PI}=$

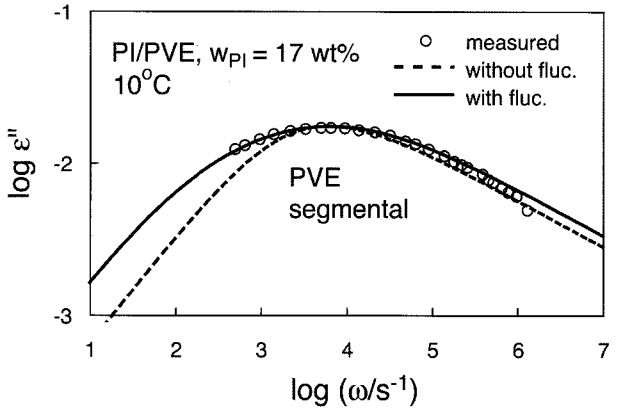

Fig. 2. Comparison of ε" data measured at 10°C for a PI/PVE blend with $M_{PI}=11.5\times10^3$, $M_{PVE}=60.2\times10^3$ and $w_{PI}=17$ wt% with prediction of Zetsche-Fischer model. Data taken from Hirose *et al.* (2003) with permission.

11.5×10^3, $M_{PVE}=60.2\times10^3$, and $w_{PI}=17$ wt% (circles). Since w_{PI} is small, the dielectric dispersion seen here is (almost) exclusively attributed to the segmental relaxation of PVE in the blend. In the bulk system of the component PVE, the dielectric segmental relaxation is satisfactorily described by the Havriliak-Negami (HN) empirical equation (Hirose *et al.*, 2004),

$$\varepsilon_{HN}''(\omega;\tau_{HN}) = -\mathrm{Im}\left\{\frac{\Delta\varepsilon}{[1+(i\omega\tau_{HN})^{\alpha}]^{\beta}}\right\} \quad \text{with } i=\sqrt{-1} \tag{6}$$

where $\Delta\varepsilon$ (=0.108) is the dielectric relaxation intensity, τ_{HN} is the HN-type nominal relaxation time, and α (=0.721) and β (=0.391) are the HN parameters for PVE. (The HN equation does not describe the real terminal behavior, $\varepsilon''\propto\omega$ at low ω, but is useful for description of the intensive part of the dielectric relaxation around the ε'' peak.) In Fig. 2, this ε_{HN}'' for bulk PVE, shifted in the double-logarithmic scale to match the ε'' peak frequency and height with the ε'' data, is shown with the dotted curve. The observed dielectric relaxation mode distribution is broader than this curve at low ω.

Hirose *et al.* (2004) interpreted this broadening as a result of concentration fluctuation. Namely, the local PVE volume fraction ϕ_{local} not only deviates from the nominal volume fraction $\phi^{[PVE]}$ because of the self concentration effect but also fluctuates in space to broaden the mode distribution. This spatial fluctuation may be described by the Zetsche-Fischer (ZF) model (1994) giving a Gaussian distribution function of ϕ_{local} around an average ϕ_o,

$$\psi(\phi_{local}) = \frac{1}{\sqrt{2\pi\sigma^2}}exp\left(-\frac{\{\phi_{local}-\phi_o\}^2}{2\sigma^2}\right) \tag{7}$$

where σ^2 is the (approximate) variance. The corresponding ε'' for PVE can be expressed as an average of $\varepsilon_{HN}''(\omega;\tau_{HN})$ over the distribution function $\psi(\phi_{local})$,

$$\varepsilon''(\omega) = \frac{\phi^{[PVE]}\int_0^1 \varepsilon_{HN}''(\omega;\tau_{HN}(\phi_{local}))\psi(\phi_{local})d\phi_{local}}{\int_0^1 \psi(\phi_{local})d\phi_{local}} \tag{8}$$

The characteristic time τ_{HN} appearing in Eq. (8) is dependent on the local volume fraction ϕ_{local}. Hirose *et al.* (2004) replaced this dependence by the dependence of the peak relaxation time τ_{peak} (=reciprocal of the peak frequency of the ε'' data) of PVE-rich PI/PVE blends on the nominal $\phi^{[PVE]}$. (In those blends, PVE dominates the dielectric signal and τ_{peak} can be safely assigned as the segmental relaxation time of PVE.) Strictly speaking, the local volume fraction ϕ_{local} corresponding to this τ_{peak} is not identical to the nominal $\phi^{[PVE]}$ but would be close to the effective $\phi_{eff}^{[PVE]}$ discussed earlier. However, a difference between $\phi^{[PVE]}$ and $\phi_{eff}^{[PVE]}$ was rather small in the PVE-rich PI/PVE blends. For this reason, the above replacement can be made as the first approximation. For the same reason, the average ϕ_o appearing in Eq. (7) can be approximated as the nominal $\phi^{[PVE]}$.

Under these approximations, Hirose *et al.* (2004) fitted the ε'' data of the PI/PVE blends with Eq. (8). (Actually, they converted ψ appearing in Eq. (8) to a distribution function of τ_{HN} to make this fit.) In Fig. 2, the solid curve indicates the best-fit result obtained with $\sigma^2=0.013$. They further analyzed this σ^2 value through a general expression for the scattering from Gaussian chains having concentration fluctuation (Zetsche and Fischer, 1994),

$$\sigma^2 = \langle\{\phi_{local}-\phi_o\}^2\rangle = \frac{b^3}{2\pi^2 r_a^2}\int_0^\infty\left\{\frac{3(sin\ qr_a - qr_a cos\ qr_a)}{q^2 r_a^2}\right\}S(q)dq \tag{9}$$

Here, b is a monomer bond length, q is the scattering vector, $S(q)$ is a structural factor, and r_a is a characteristic length of the concentration fluctuation. Utilizing an expression of $S(q)$ based on the random phase approximation (known to be valid for blends and diblock copolymers; de Gennes, 1979), Hirose *et al.* evaluated r_a from the σ^2 value (=0.013). The result, $r_a=1.6$~1.7 nm, agreed well with the segment size estimated by using the dielectric data of PI as the reference, $r_{seg}=1.8\pm0.3$ nm, and was reasonably close to the Kuhn segment length of PVE, $b_K=1.16$ nm. This result lends further support for the molecular picture that the Kuhn segment behaves as the dielectrically detected monomeric segment.

3. Global dynamics

3.1. Application of tube model

The global motion of polymer chains (over the end-to-end distance) governs their terminal relaxation and flow behavior. For entangled homopolymer systems, this motion

and the corresponding dynamic properties have been analyzed in terms of various versions of the tube model (Watanabe, 1999; McLeish, 2002). For miscible blends composed of high-M, entangling chains, attempts have been made to modify the tube model and describe the terminal relaxation behavior (Pathak *et al.*, 2004; Haley *et al.*, 2003, 2005). In this modification, the friction coefficients ζ of the Rouse segments (motional unit for the terminal relaxation) of the component chains are evaluated from the effective T_g^{eff} on the basis of the self concentration concept, and the entanglement length (or tube diameter), a, is estimated from some blending law. The parameters ζ and a thus obtained are utilized to evaluate the characteristic times/intensities for the relaxation mechanisms established in the tube model (reptation, length fluctuation, constraint release, *etc.*) thereby formulating the relaxation modulus $G(t)$ for the entangled miscible blends.

For miscible PI/PVE blends, Pathak *et al.* (2004) evaluated the WLF-type friction coefficients ζ_{PI}, ζ_{PVE} for the Rouse segments of PI and PVE based on respective T_g^{eff}. In addition, they assumed that the entanglement length was common for PI and PVE therein to specify a_{blend} in the blend from a harmonic blending rule, $1/a_{blend}=\phi^{[PI]}/a_{PI}+\phi^{[PVE]}/a_{PVE}$. Utilizing these ζ and a, they proposed an expression of $G(t)$ on the basis of the double-reptation model (des Cloizeaux, 1990),

$$G(t)=G_N\{\phi^{[PI]}F_{PI}(t)+\phi^{[PVE]}F_{PVE}(t)\}^2 \quad (10)$$

Here, G_N is the entanglement plateau modulus: $G_N=\rho RT/M_e$ where ρ, R, T are the blend density, gas constant, absolute temperature, respectively. M_e included in this expression of G_N is the entanglement molecular weight in the blend evaluated from a_X and $M_e^{[X]}$ of the component X (= PI, PVE) in bulk and a_{blend} in the blend as $M_e=\{a_{blend}/a_X\}^2 M_e^{[X]}$. $F_X(t)$ appearing in Eq. (10) represents the survival probability of the entanglement for the component X at time t in the blend. Within the context of the double-reptation model, $F_X(t)$ is evaluated from the survival probability for the component X in bulk, $F_X^0(t)=\{G^{[bulk\ X]}(t)/G_N^{[bulk\ X]}\}^{1/2}$ after correcting the relaxation time for differences of ζ and a in the blend and bulk (Pathak *et al.*, 2004).

The prediction of the model proposed by Pathak *et al.* (2004) is fairly close to the data for the entangled PI/PVE blends in short time scales where the slow component (PVE) has hardly relaxed. However, in the terminal relaxation regime, the model predicts slower and weaker relaxation compared to the data. This difference (by a factor of ~3 for both of the terminal relaxation times and intensity) may be attributable to the problem of the double-reptation model itself. Namely, this model assumes that the entanglement is a binary interaction and the stress relaxes immediately on removal of the entanglement. However, the stress relaxation actually requires motion of the chain after the entanglement removal, and the double-reptation model works approximately only when the time necessary for this motion is negligible (Watanabe, 1999). In addition, there remains some uncertainty in the harmonic blending rule for the entanglement length a adopted by Pathak *et al.*, as discussed later for blends of PI and poly(*p-tert*-butyl styrene). This uncertainty may be also responsible for the difference between their model prediction and the data for the PI/PVE blends.

Haley *et al.* (2003, 2005) proposed a model based on a molecular picture of dynamic tube dilation, the picture being more sophisticated than the picture of double-reptation. Their model reasonably describes the data for PI/PVE blends but non-trivial deviation still remains. This deviation may be attributable to a problem in formulation of the tube dilation process itself (that has been fully discussed for PI/PI binary blends; Watanabe *et al.*, 2004a, 2004b, 2006). Obviously, the dynamics in miscible blends can be accurately described only after the homopolymer dynamics is well understood. Thus, further studies of the entanglement in homopolymer systems are necessary for our better understanding of the miscible blend dynamics.

3.2. Effect of dynamic heterogeneity on terminal relaxation

In general, the time-temperature superposition fails for a miscible A/B blend as a whole because of a difference of the temperature dependence of their segmental friction coefficients ζ_A and ζ_B of the components (that reflects the difference of their effective T_g^{eff}). However, respective component chains may obey this superposition. For example, the PI chain in the PI/PVE blend examined in Fig. 1 shows good superposition in both segmental and global relaxation regimes. However, this thermo-rheological simplicity does not always hold for the component chains if they have a large dynamic asymmetry, as revealed from recent studies for miscible blends of PI and poly(*p-tert*-butyl styrene) (Watanabe *et al.*, 2007; Takada *et al.*, 2008; Chen *et al.*, 2008). The characteristic features of the PI/PtBS blends are summarized below.

3.2.1. Thermo-rheological behavior

PI and poly(*p-tert*-butyl styrene) (PtBS) exhibit the LCST phase behavior with a very high T_{LCST} (250°C for M_{PI}, $M_{PtBS}\sim10^5$; Watanabe *et al.*, 2007), as found in scattering experiments by Yurekli and Krishnamoorti (2004). Furthermore, PI has the type-A dipole while PtBS does not, which enables us to dielectrically examine the global dynamics of PI in the miscible PI/PtBS blends. These features are similar to those of the PI/PVE blends examined in the previous section. However, the frictional asymmetry is much higher for the PI/PtBS blends than for the PI/PVE blends, as noted from bulk T_g of the components; T_g/°C ≅ −70, 0, and 150 for PI, PVE, and PtBS, respectively. This large asymmetry in the PI/PtBS blends

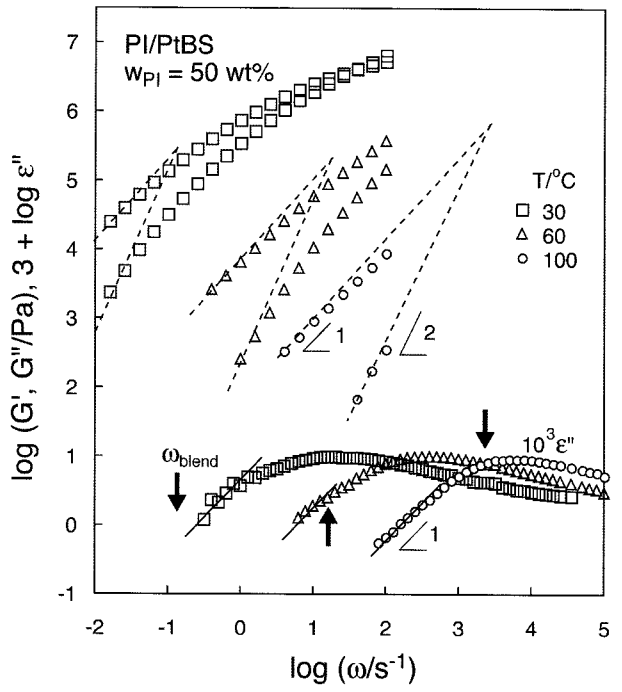

Fig. 3. Viscoelastic and dielectric behavior of a PI/PtBS blend with $M_{PI}=19.9\times10^3$, $M_{PtBS}=16.4\times10^3$, and $w_{PI}=50$ wt% at temperatures as indicated. Data taken from Chen *et al.* (2008) with permission.

magnifies the effect of dynamic heterogeneity on the component dynamics.

As an example, Fig. 3 shows ω dependence of the viscoelastic storage and loss moduli, G' and G'', and the dielectric loss, ε'', measured for a PI/PtBS blend with $M_{PI}=19.9\times10^3$, $M_{PtBS}=16.4\times10^3$, and $w_{PI}=50$ wt% (Chen *et al.*, 2008). The data are shown only at representative temperatures in the miscible regime (well below T_{LCST}), and the ε'' data are multiplied by a factor of 10^3 for easy comparison with the G' and G'' data. (The ε'' data at low ω were dominated by direct current conductivity of ionic impurities and not shown here.) As judged from the blend composition and the entanglement molecular weight in bulk, $M_e^{[PI]}=5.0\times10^3$ for PI (Ferry, 1980) and $M_e^{[PtBS]}=37.6\times10^3$ for PtBS (Fetters *et al.*, 2007), the PI chains are entangled in bulk as well in the blend while the PtBS chains are non-entangled in bulk. However, in the blend, the PtBS chains appear to be topologically constrained (or entangled) by the PI chains, as discussed later.

In Fig. 3, we note the viscoelastic and dielectric terminal relaxation behavior characterized with the power-law tails, $G'\propto\omega^2, G''\propto\omega$, and $\varepsilon''\propto\omega$. This behavior is observed in our experimental window because PtBS (being glassy in bulk state) is significantly plasticized by PI. Correspondingly, PI is anti-plasticized by PtBS.

Obviously, all components in the blend (PI and PtBS) contribute to G' and G''. In contrast, the ε'' data shown in Fig. 3 detect only the global dynamics of PI having the type-A dipole. (The segmental relaxation of PI and PtBS occurs at high ω not covered in Fig. 3.) Thus, comparison of the viscoelastic and dielectric data enables us to specify the fast and slow components in the blend. For this purpose, the terminal viscoelastic relaxation frequency of the blend, $\omega_{blend}=[\omega G''/G']_{\omega\to0}$, are shown with the arrows in Fig. 3. At low T, this ω_{blend} is much smaller than the ε'' peak frequency $\omega_{\varepsilon\text{-peak}}$ and located in a range of ω where the terminal tail of $\varepsilon''(\propto\omega)$ is observed. Thus, PI relaxes much faster than the blend as a whole, which enables us to assign PI and PtBS as the fast and slow components at low T. In contrast, at high T, ω_{blend} becomes closer to $\omega_{\varepsilon\text{-peak}}$ and thus the PI relaxation rate becomes close to the PtBS relaxation rate. This change of the relative relaxation rates of PI and PtBS with T is mainly due to a difference of their effective T_g^{eff} : $T_g^{eff}=-37$°C and 10°C for PI and PtBS examined in Fig. 3 (these T_g^{eff} values were obtained from WLF analysis of shift factors; Chen *et al.*, 2008). Thus, the WLF type acceleration of the relaxation is stronger for PtBS (having a higher T_g^{eff}) than for PI, which reduces the difference of the relaxation rates of PI and PtBS with increasing T.

Fig. 4 examines the thermo-rheological behavior of PI in the blend. For this purpose, the ε'' data exclusively detecting the global motion of PI are shifted along the ω axis to achieve the best superposition on the data at a reference temperature, T_r = 120°C. (A minor change of the dielectric intensity with T has been corrected by a factor, $b_T=T/T_r$ with T and T_r in K unit, multiplied to the ε'' data.) The solid curve indicates the ε'' data of bulk PI multiplied by the PI volume fraction in the blend and further sifted along the ω axis to mach the ε'' peak frequency $\omega_{\varepsilon\text{-peak}}$ with that of PI in the blend. We note that the superposition works excellently at $\omega\geq\omega_{\varepsilon\text{-peak}}$ but not at lower $\omega<\omega_{\varepsilon\text{-peak}}$. Specifically, an extra slow relaxation process emerges at low T while at high T this process vanishes and the PI data in the blend agree with the bulk PI data (solid curve).

This thermo-rheological complexity of PI can be related to the dynamic heterogeneity in the blend, as discussed by

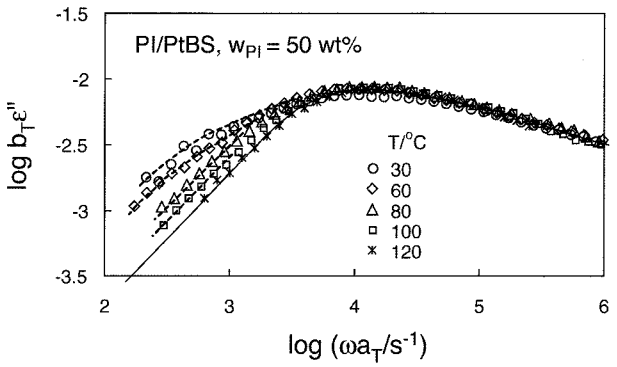

Fig. 4. Test of time-temperature superposability for PI chains in PI/PtBS blend with $M_{PI}=19.9\times10^3$, $M_{PtBS}=16.4\times10^3$, and $w_{PI}=50$ wt%. The reference temperature is $T_r=120$°C. Data taken from Chen *et al.* (2008) with permission.

Watanabe *et al.* (2007) and Chen *et al.* (2008): In the blend examined in Fig. 3, the concentration C_{PtBS} of PtBS (the slow component at low T) is not much larger than its overlapping concentration C_{PtBS}^* ($C_{PtBS}/C_{PtBS}^* = 2.3$), and the average end-to-end distance R_{PI} of PI (the fast component) is fairly close to R_{PtBS} of PtBS (R_{PI}/R_{PtBS} 1.6). Under these conditions, all PI chains cannot simultaneously have the same degree of overlapping with the PtBS chains, meaning that the PI chains in a PtBS-rich region feel a higher friction compared to the other PI chains. This frictional nonuniformity survives during the global relaxation of PI at low T because PtBS relaxes much slower than PI at low T. Then, the ensemble of PI chains is composed of the minority (slow PI in the PtBS-rich region) and majority (fast PI), and the former gives the extra slow relaxation at low T. On the other hand, at high T, PtBS relaxes equally fast compared to PI so that the frictional nonuniformity tends to be smeared during the global relaxation of PI. In addition, the difference of the relaxation rates of the minority and majority PI becomes smaller with increasing T (because the minority in the PtBS-rich region has a higher T_g^{eff} compared to the majority and the WLF type acceleration of the relaxation is stronger for the minority). The thermo-rheological complexity seen in Fig. 4 is mainly attributable to this change of the behavior of the minority PI with T.

From the above argument, we expect that the PI chains exhibit the thermo-rheological simplicity in a given range of T where they relax slower than PtBS chains. This expectation has been confirmed by Takada *et al.* (2008) for a PI/PtBS blend with M_{PI} and M_{PtBS} being identical to those of the blend examined in Fig. 3 but with a smaller $w_{PtBS} = 20$ wt%. (In this 20 wt% blend, the PtBS chains were very strongly plasticized thereby relaxing faster than the PI chains.)

In relation to the above argument, we should also note that the PI chains in the PI/PVE blend examined in Fig. 1 exhibit no thermo-rheological complexity in the global relaxation regime. This fact can be related to a smaller dynamic asymmetry for a pair of PI and PVE (compared to the pair of PI and PtBS) as well as the molecular weight of the slow component (PVE) in the PI/PVE blend: Those high-M PVE chains are rather heavily overlapping in the blend thereby giving an uniform frictional environment for PI chains.

Now, we turn our attention to the thermo-rheological behavior of PtBS in the PI/PtBS blend. For entangled PI, a ratio of the viscoelastic terminal relaxation time τ_G to the dielectric terminal relaxation time τ_ε changes a little with a change in the contribution of the constraint release (CR) and dynamic tube dilation (DTD) mechanisms to the relaxation; $\tau_G/\tau_\varepsilon = 1$ and 1/2 for the cases of no and full contribution of CR/DTD (Watanabe, 1999). Chen *et al.* (2008) utilized the dielectric τ_ε of PI ($\tau_\varepsilon = 1/\omega_{\varepsilon\text{-peak}}$ in the terminal regime) as a reference time for the viscoelastic relaxation of PI to evaluate the viscoelastic modulus G_{PI}^* of PI in the blend from the G^* data of bulk PI after a minor correction for the CR/DTD effect on the τ_G/τ_ε ratio. Furthermore, they subtracted this G_{PI}^* from the G^* data of the blend to evaluate the modulus G_{PtBS}^* of PtBS in the blend. The time-temperature superposability of this G_{PtBS}^* is examined in Fig. 5, where the G_{PtBS}^* data obtained at various T are reduced by the intensity correction factor b_T ($= T/T_r$ with T, T_r in K unit) and shifted along the ω axis to achieve the best superposition on the data at $T_r = 120$°C (Chen *et al.*, 2008). The dotted curves indicate the data for bulk PtBS reduced at the iso-frictional state explained later. We note that the superposition works considerably well for the G_{PtBS}^* data. This thermo-rheological simplicity of PtBS in the blend can be related to the motion of the PI chains. Namely, the frictional nonuniformity (existing at low T) has been smeared in the terminal relaxation process of PtBS because of the fast motion of PI. Thus, all PtBS chains possibly feel the same friction thereby exhibiting the thermo-rheological simplicity.

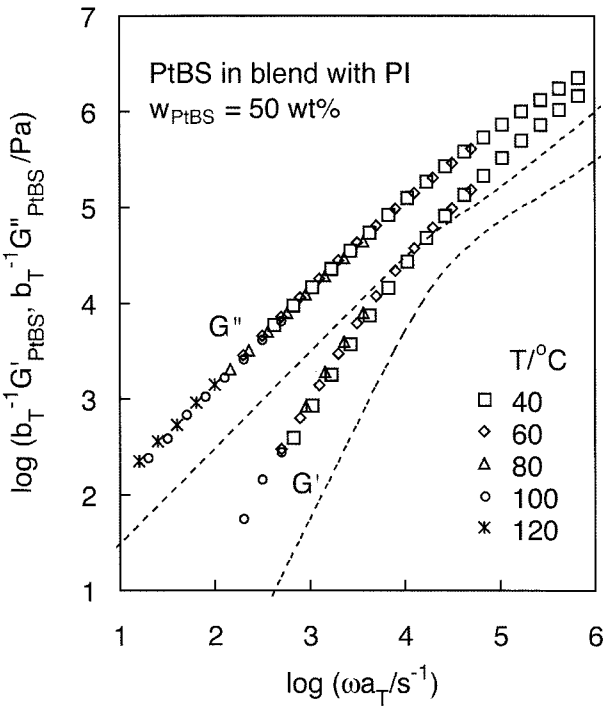

Fig. 5. Test of time-temperature superposability for PtBS chains in PI/PtBS blend with $M_{PI} = 19.9\times10^3$, $M_{PtBS} = 16.4\times10^3$, and $w_{PI} = 50$ wt%. The reference temperature is $T_r = 120$°C. Data taken from Chen *et al.* (2008) with permission.

3.2.2. Entanglement in miscible blend

Chen *et al.* (2008) made WLF analysis of the shift factor a_T utilized in Fig. 4 to determine the *iso-frictional* temperature for PI (the majority giving the ε" peak), $T_{iso} = 63$°C, being defined with respect to bulk PI at $T_{iso} = 30$°C. They also made the WLF analysis of the a_T factor utilized in Fig. 5 to determine T_{iso} (=43°C) for PtBS in the blend

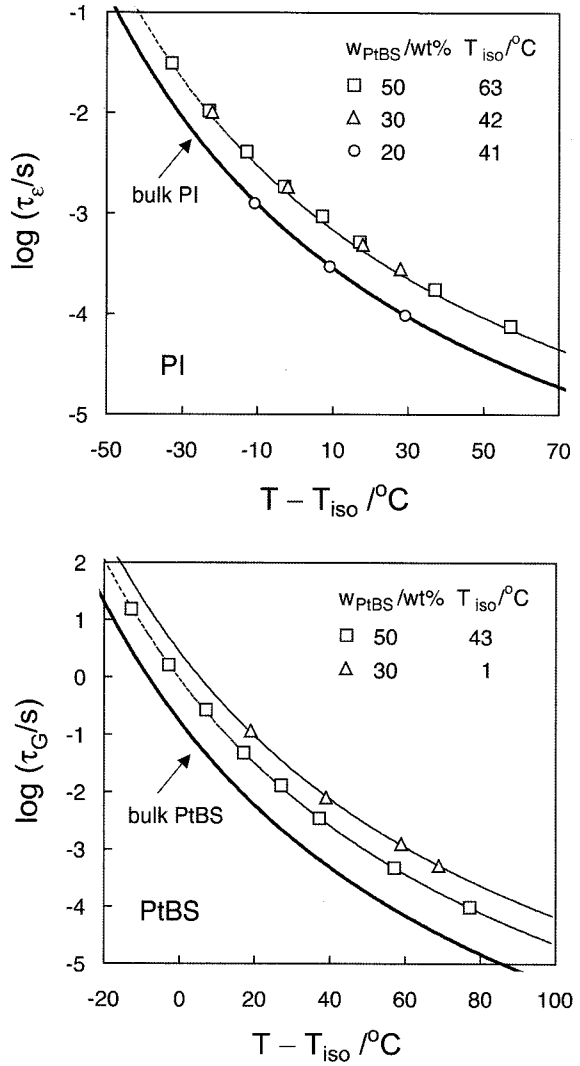

Fig. 6. Comparison of relaxation times of PI and PtBS in PI/PtBS blend ($M_{PI}=19.9\times10^3$, $M_{PtBS}=16.4\times10^3$) with those in respective iso-frictional bulk states. Data taken from Chen *et al.* (2008) with permission.

defined with respect to bulk PtBS at $T_{iso}^{bulk\ PtBS}=171$°C. The relaxation time of the Rouse segment (motional unit for the global relaxation) of either PI or PtBS chain is the same in the blend at a temperature T and in bulk at $T=T-\Delta T_{iso}$ with $\Delta T_{iso}=T_{iso}-T_{iso}^{bulk}$.

For the PI/PtBS blend with $M_{PI}=19.9\times10^3$, $M_{PtBS}=16.4\times10^3$, and $w_{PI}=50$ wt% (examined in Figs. 3~5), the dielectric terminal relaxation time of the majority PI therein, $\tau_\varepsilon(=1/\omega_{\varepsilon\text{-peak}})$, is plotted against and a distance from the iso-frictional temperature, $T-T_{iso}$, in the top panel of Fig. 6 (see squares). The plots of the viscoelastic terminal relaxation time of PtBS in that blend, $\tau_G(=[G_{PtBS}'/\omega G_{PtBS}'']_{\omega\to0})$; evaluated from the G_{PtBS}* data shown in Fig. 5), are shown with the squares in the bottom panel. For comparison, the plots are shown also for the PI/PtBS blends with the same M_{PI} and M_{PtBS} but smaller w_{PI} as well as for bulk PI and PtBS (Chen *et al.*, 2008; Takada *et al.*, 2008).

In the top panel of Fig. 6, the dotted curve indicates the τ_ε data of bulk PI multiplied by a factor of 2.4. The τ_ε data in the blends with $w_{PtBS}=30$ and 50 wt% are close to this dotted curve and thus larger, by a factor of 2.4, than τ_ε in the iso-frictional bulk system. This behavior of PI chains in the blends can be related to topological constraint (or entanglement) from the slow PtBS chains. Namely, M_{PtBS} of the PtBS chains is smaller than $M_e^{[PtBS]}$ ($=37.6\times10^3$) of bulk PtBS and these chains cannot entangle by themselves, but they still behave as immobilized short threads during the global relaxation of PI thereby constrain the PI motion. In relation to this point, we note that τ_ε in the blend with $w_{PtBS}=20$ wt% is close to that in the iso-frictional bulk. In this blend, PtBS relaxed faster than PI and thus the entanglement mesh between the PI chains would have been *diluted* by the PtBS chains. As judged from the agreement of τ_ε in this diluted PI-PI entanglement mesh and undiluted mesh in bulk, the PI motion in the diluted mesh appears to be still constrained by the PtBS chains, which is in harmony with the above argument for the blends with $w_{PtBS}=30$ and 50 wt%.

Now, we turn our attention to the behavior of PtBS chains shown in the bottom panel of Fig. 6. The thin solid and dotted curves, respectively, indicate the τ_G data of iso-frictional PtBS bulk (thick solid curve) multiplied by factors of 15.8 and 5.4. The τ_G data of the PtBS chains in the blends with $w_{PtBS}=30$ and 50 wt% are close to these curves, indicating that the PtBS relaxation is significantly retarded by the PI chains. This retardation is noted also in Fig. 5 where the bulk PtBS data reduced at the iso-frictional temperature are shown with the dotted curves. The PtBS relaxation is considerably slower in the blend than in the iso-frictional bulk. Thus, the PtBS relaxation in the blends is *topologically constrained* by the PI chains. This topological constraint (or entanglement) for the PtBS chains due to the PI chains may be a natural consequence of the entanglement criterion, as discussed below.

For bulk homopolymers, this criterion can be characterized by the number P_e of entanglement strands within a volume a^3, where a is the entanglement length (or the tube diameter within the context of the tube model). This P_e is nearly constant for a variety of flexible homopolymers including PI and PtBS (Fetters *et al.*, 2007):

$$P_e\equiv\frac{a^3}{V_e}=\frac{a}{p}=20\pm3 \tag{11}$$

In Eq. (11), V_e denotes the occupied volume of the entanglement strand; $V_e=M_e/(\rho N_A)$ with ρ and N_A being the polymer density and Avogadro constant. p is the packing length defined as a ratio of the occupied volume of the Kuhn segment υ_0 to square of the Kuhn length b_K (Fetters *et al.*, 1994, 1999, 2007):

$$p\equiv\frac{\upsilon_0}{b_K^2} \tag{12}$$

Utilizing the criterion, Eq. (11), we can examine if the low-M PtBS chains ($M_{PtBS}=16.4\times10^3\cong0.4M_e^{[PtBS]}$) can be topologically constrained by the PI chains. For this purpose, we may estimate an effective packing length in the blends as an average,

$$p_{blend}=n_{PtBS}\,p_{PtBS}+n_{PI}\,p_{PI} \quad (13)$$

Here, n_{PtBS} and n_{PI} denote the number fractions of the Kuhn segments of PtBS and PI in the blends, and p_{PtBS} (= 0.48_1 nm) and p_{PI} (=0.26_9 nm) are the intrinsic packing lengths of PtBS and PI reported in literature (Fetters, 2007). Since the molecular weight of the Kuhn segment M_K is considerably larger for PtBS ($M_{K,PtBS}\cong1500$) than for PI ($M_{K,PI}\cong130$), n_{PtBS} is much smaller than n_{PI} to give $p_{blend}\cong p_{PI}$; $n_{PtBS}=0.036$ and 0.080 and $p_{blend}=0.27_7$ and 0.28_6 nm for the PI/PtBS blends with $w_{PtBS}=30$ and 50 wt%, respectively (Chen *et al.*, 2008). Correspondingly, the effective entanglement length estimated from Eq. (11), $a_{blend}\cong20p_{blend}$, is not very different from a_{PI} (=5.1 nm) for bulk PI; $a_{blend}=5.5$ and 5.7 nm for $w_{PtBS}=30$ and 50 wt%, respectively.

These a_{blend} values are smaller than the average end-to-end distance of the PtBS chain with $M_{PtBS}=16.4\times10^3$, R_{PtBS} =7.7 nm (evaluated from an empirical equation, $R_{PtBS}=0.0601\times M_{PtBS}^{1/2}$; Fetters *et al.*, 2007), suggesting that the PtBS chain is short but still topologically constrained by the PI chains. The PI segments have a large, average volume fraction of in a random coil of each PtBS chain (ϕ_{PI}= 0.53 and 0.73 in the blends with $w_{PtBS}=50$ and 30 wt%), and the PI backbone is much more flexible compared to the PtBS backbone. Thus, each random coil of PtBS seems to acquire a much longer contour of chain backbone in it when blended with PI, which possibly results in the topological constraint for the PtBS chains (somewhat similar to the usual entanglement). Although the difference between a_{blend} and R_{PtBS} is not very large, moderate overlapping of neighboring PtBS chains ($C_{PtBS}/C_{PtBS}^*=1.4$ and 2.3 for $w_{PtBS}=30$ and 50 wt%) should enhance this constraint to significantly retard the PtBS relaxation. PI chains stitch neighboring random coils of PtBS, which also enhances this constraint (Chen *et al.*, 2008). Concerning this enhancement due to the PI chains, we expect that the PtBS relaxation is activated by the motion of the PI chains. This relaxation mechanism, not identical to but somewhat similar to the usual constraint release mechanism (Chen *et al.*, 2008), deserves further study.

Finally, we note that the harmonic blending rule of the entanglement length proposed by Pathak *et al.* (2004), $1/a_{blend}=\phi^{[A]}/a_A+\phi^{[B]}/a_B$, gives $a_{blend}=6.7$ and 7.6 nm for the PI/PtBS blends with $w_{PtBS}=30$ and 50 wt%, respectively. These a_{blend} values are just comparable to the R_{PtBS} value (= 7.7 nm) and do not appear to be consistent with the significant retardation observed for the PtBS chain in the PI/PtBS blends. Thus, the entanglement length estimated on the basis of the packing length (Eqs. 11 and 13) seems to better describe the topological constraint in miscible blends. However, the validity of this estimate has not been fully proven from molecular analysis. A further study is desired for this issue.

4. Concluding remarks

We have presented a brief summary for the segmental and global dynamics of component chains in miscible blends. The segmental dynamics is strongly affected by the self concentration reflecting the chain connectivity and also by the concentration fluctuation and the torsional barrier in respective chains, which leads to broad glass transition and the thermo-rheological complexity of the blend as a whole. The global dynamics is mainly affected by the dynamic asymmetry of the component chains. Specifically, this asymmetry can lead to the thermo-rheological complexity of the global dynamics of the fast component chains given that the slow component chains are not heavily overlapping with each other and the fast component chains are comparable/smaller, in size, compared to the slow component chains. The entanglement between such component chains, being somewhat similar but not identical to the usual entanglement of bulk homopolymers, deserves further study.

Acknowledgements

This work was partly supported by Grant-in-Aid for Scientific Research on Priority Area "Soft Matter Physics" from the Ministry of Education, Culture, Sports, Science and Technology (grant #18068009) and by Grant-in-Aid for Scientific Research B from the Japan Society for the Promotion of Science (grant # 21350126).

References

Alegria, A., J. Colmenero, K. L. Ngai and C. M. Roland, 1994, Observation of the component dynamics in a miscible polymer blend by dielectric and mechanical spectroscopies, *Macromolecules* **27**, 4486.

Chen, Q., Y. Matsumiya, Y. Masubuchi, H. Watanabe and T. Inoue, 2008, Component Dynamics in Polyisoprene/Poly(4-tert-butylstyrene) Miscible Blends, *Macromolecules* **41**, 8694-8711.

Chung, G. C., J. A. Kornfield and S. D. Smith, 1994, Component dynamics in miscible polymer blends – a 2-dimensional deuteron NMR investigation, *Macromolecules* **27**, 964.

Des Cloizeaux, J., 1990, Relaxation and viscosity anomaly of melts made of long entangled polymers - Time-dependent reptation, *Macromolecules* **23**, 4678.

Ediger, M. D., T. R. Lutz and Y. He, 2006, Dynamics in glass-forming mixtures: Comparison of behavior of polymeric and non-polymeric components, *J. Non-cyrst. Solids* **352**, 4718.

Endoh, M. K., M. Takenaka, T. Inoue, H. Watanabe and T. Hash-

imoto, 2008, Shear small-angle light scattering studies of shear-induced concentration fluctuations and steady state viscoelastic properties, *J. Chem. Phys.* **128**, Article # 164911.

Ferry, J. D., 1980, Viscoelastic Properties of Polymers, Third ed., Wiley, New York.

Fetters, L. J., D. J. Lohse, D. Richter, T. A. Witten and A. Zirkel, 1994, Connection between polymer molecular-weight, density, chain dimensions, and melt viscoelastic properties, *Macromolecules* **27**, 4639.

Fetters, L. J., D. J. Lohse and W. W. Graessley, 1999, Chain dimensions and entanglement spacings in dense macromolecular systems, *J. Polym. Sci. Part B: Polym. Phys.* **37**, 1023.

Fetters, L. J., D. J. Lohse and R. H. Colby, 2007, Chain Dimensions and Entanglement Spacings, in Physical Properties of Polymer Handbook (2nd edition), Mark, J. E. ed., Springer, New York.

De Gennes, P. G., 1979, Scaling Concept in Polymer Physics, Cornell Univ. Press, Ithaca.

Haley, J. C., T. P. Lodge, Y. Y. He, M. D. Ediger, E. D. von Meerwall and J. Mijovic, 2003, Composition and temperature dependence of terminal and segmental dynamics in polyisoprene/poly(vinylethylene) blends, *Macromolecules* **36**, 6142.

Haley, J. C. and T. P. Lodge, 2005, Viscosity predictions for model miscible polymer blends: Including self-concentration, double reptation, and tube dilation, *J. Rheol.* **49**, 1277.

Hirose, Y., O. Urakawa and K. Adachi, 2003, Dielectric study on the heterogeneous dynamics of miscible polyisoprene/poly (vinyl ethylene) blends: Estimation of the relevant length scales for the segmental relaxation dynamics, *Macromolecules* **36**, 3699.

Hirose, Y., O. Urakawa and K. Adachi, 2004, Dynamics in disordered block copolymers and miscible blends composed of poly(vinyl ethylene) and polyisoprene, *J. Polym. Sci. Part B: Polym. Phys.* **42**, 4084.

Inoue, T., Uemtasu, T. and Osaki, K., 2002, The significance of the Rouse segment: Its concentration dependence, *Macromolecules* **35**, 820.

Kanaya T. and K. Kaji, 2001, Dynamics in the glassy state and near the glass transition of amorphous polymers as studied by neutron scattering, *Adv. Polym. Sci.* **154**, 87.

Kumar, S. K., R. H. Colby, S. H. Anastasiadis and G. Fytas, 1996, Concentration fluctuation induced dynamic heterogeneities in polymer blends, *J. Chem. Phys.* **105**, 3777.

Lodge, T. P. and T. C. B. McLeish, 2000, Self-concentrations and effective glass transition temperatures in polymer blends, *Macromolecules* **33**, 5278.

Lutz, T. R., Y. He, M. D. Ediger, M. Pitsikalis and N. Hadjichristidis, 2004, Dilute polymer blends: Are the segmental dynamics of isolated polyisoprene chains slaved to the dynamics of the host polymer?, *Macromolecules* **37**, 6440.

McLeish, T. C. B, 2002, Tube theory of entangled polymer dynamics, *Adv. Phys.* **51**, 1379.

Miller J. B., K. J. McGrath, C. M. Roland, C. A. Trask and A. N. Garroway, 1990, Nuclear-magnetic-resonance study of polyisoprene poly(vinylethylene) miscible blends, *Macromolecules* **23**, 4543.

Miura, N., W. J. MacKnight, S. Matsuoka and F. E. Karasz, 2001, Comparison of polymer blends and copolymers by broadband dielectric analysis, *Polymer* **42**, 6129.

Pathak, J. A., R. H. Colby, S. Y. Kamath, S. K. Kumar and R. Stadler, 1998, Rheology of miscible blends: SAN and PMMA, *Macromolecules* **31**, 8988.

Pathak, J. A., R. H. Colby, G. Floudas and R. Jerome, 1999, Dynamics in miscible blends of polystyrene and poly(vinyl methyl ether), *Macromolecules* **32**, 2553.

Pathak, J. A., S. K. Kumar and R. H. Colby, 2004, Miscible polymer blend dynamics: Double reptation predictions of linear viscoelasticity in model blends of polyisoprene and poly(vinyl ethylene), *Macromolecules* **37**, 6994.

Takada, J., H. Sasaki, Y. Matsushima, A. Kuriyama, Y. Matsumiya, H. Watanabe, K. H. Ahn and W. Yu, 2008, Component chain dynamics in a miscible blend of low-M poly(p-t-butyl styrene) and polyisoprene, *Nihon Reoroji Gakkaishi* (*J. Soc. Rheol. Japan*) **36**, 35.

Takenaka, M., S. Nishitsuji, T. Taniguchi, M. Yamaguchi, K. Tada and T. Hashimoto, 2006, Computer simulation study on the shear-induced phase separation in semidilute polymer solutions in 3-dimensional space, *Polymer* **47**, 7846.

Tomlin D. W. and C. M. Roland, 1992, Negative excess enthalpy in a Van der Waals polymer mixture, *Macromolecules* **25**, 2994.

Urakawa O., 2004, Studies on dynamic heterogeneity in miscible polymer blends and dynamics of flexible polymer, *Nihon Reoroji Gakkaishi* (*J. Soc. Rheol. Japan*) **32**, 265.

Utracki, L. A., 1989, Polymer Alloys and Blends, Carl Hanser Verlag, Munich.

Watanabe, H., 1999, Viscoelasticity and dynamics of entangled polymers, *Prog. Polym. Sci.* **24**, 1253.

Watanabe, H. 2001, Dielectric relaxation of type-A polymers in melts and solutions, *Macromol. Rapid Commun.* **22**, 127.

Watanabe, H., S. Ishida, Y. Matsumiya and T. Inoue, 2004a, Viscoelastic and dielectric behavior of entangled blends of linear polyisoprenes having widely separated molecular weights: Test of tube dilation picture, *Macromolecules* **37**, 1937.

Watanabe, H., S. Ishida, Y. Matsumiya and T. Inoue, 2004b, Test of full and partial tube dilation pictures in entangled blends of linear polyisoprenes, *Macromolecules* **37**, 6619.

Watanabe, H., T. Sawada and Y. Matsumiya, 2006, Constraint release in star/star blends and partial tube dilation in monodisperse star systems, *Macromolecules* **39**, 2553.

Watanabe, H., Y. Matsumiya, J. Takada, H. Sasaki, Y. Matsushima, A. Kuriyama, T. Inoue, K. H. Ahn, W. Yu and R. Krishnamoorti, 2007, Viscoelastic and dielectric behavior of a polyisoprene/poly(4-tert-butyl styrene) miscible blend, *Macromolecules* **40**, 5389.

Yurekli K. and R. Krishnamoorti, 2004, Thermodynamic interactions in blends of poly(4-tert-butyl styrene) and polyisoprene by small-angle neutron scattering, *J. Polym. Sci. Part B: Polym. Phys.* **42**, 3204.

Zetsche, A. and E. W. Fischer, 1994, Dielectric studies of the alpha-relaxation in miscible polymer blends and its relation to concentration fluctuations, *Acta Polym.* **45**, 168.

Zhao, J., L. Zhang and M. D. Ediger, 2008, Poly(ethylene oxide) Dynamics in Blends with Poly(vinyl acetate): Comparison of Segmental and Terminal Dynamics, *Macromolecules* **41**, 8030.